American Mineralogist, Volume 100, pages 2185–2190, 2015

Water effects on the anharmonic properties of forsterite

YAN YANG[1,*], ZHONGPING WANG[2], JOSEPH R. SMYTH[3], JIA LIU[1] AND QUNKE XIA[1]

[1]CAS Key Laboratory of Crust-Mantle Materials and Environments, School of Earth and Space Sciences, University of Science and Technology of China, Hefei 230026, China
[2]Physics Experiment Teaching Centers, University of Science and Technology of China, Hefei 230026, China
[3]Department of Geological Sciences, University of Colorado, Boulder, Colorado 80309, U.S.A.

ABSTRACT

To quantify the effects of hydration on anharmonicity of olivine thermodynamics, we have measured in situ Raman spectra of an extremely hydrous forsterite with 4500 ppm (wt) H_2O at temperatures up to 1273 K. All the Raman modes in hydrous forsterite shift linearly to lower wavenumbers with increasing temperature. The calculated isobaric mode Grünesien parameters related to SiO_4 internal stretching and bending vibrations are much lower than lattice vibrations. Additionally, compared with anhydrous forsterite, except for the modes at 919, 858, and 227 cm^{-1}, water greatly reduces the isobaric mode Grüneisen parameters of the Raman modes in forsterite. Water also has a large effect on the anharmonic parameters related to lattice vibrations, whereas it has little effect on the anharmonic parameters related to SiO_4 internal stretching and bending vibrations. Those results have the implications to the variations of local structure with temperature and estimation of water effects on the thermodynamics of forsterite.

Keywords: Water, anharmonic properties, Raman mode, forsterite

INTRODUCTION

Olivine is a major constituent of the upper mantle (Akimoto et al. 1976). It is known to contain significant amounts of water as OH defects in the structure and can be considered as a large reservoir of water in the upper mantle (Bell and Rossman 1992; Bolfan-Casanova 2005; Beran and Libowitzky 2006; Koch-Müller et al. 2006). The presence of water in olivine has a profound influence on the physical properties of olivine, thereby on the dynamics of the upper mantle (Hirth and Kohlstedt 1996; Jung and Karato 2001; Mei and Kohlstedt 2000; Karato 2006; Wang 2010). Moreover, water has great effects on structure and thermal expansion of olivine (Smyth et al. 2006; Ye et al. 2009). However, it is not clear whether water affects such thermodynamic functions as heat capacity and entropy. Direct measurements of those thermodynamic properties of the minerals under deep earth conditions are difficult (Gillet et al. 1991, 1997; Fujimori et al. 2002), so it is desirable to have another method for estimating those properties. One of the important contributions of vibrational spectroscopy is the calculation of those thermodynamic functions (Kieffer 1979).

The lattice anharmonicity refers to the vibrational effects that do not follow simple harmonic motion. It is indispensable to understand such ubiquitous phenomena as thermal expansion and thermal conductivity, which cannot be explained in a harmonic system. Moreover, anharmonicity is especially remarkable and can dramatically modify the thermodynamic properties of material at high temperature (e.g., Karki et al. 2000; Wu 2015). So understanding anharmonic effects is one of the current problems in physics and draws more and more interests from physicists and geophysicists (e.g., Gillet et al. 1991, 1997; Fujimori et al. 2002; Zucker and Shim 2009; Deshpande et al. 2014; Silva et al. 2014; Sumita and Yoneda 2014; Wu 2015). Because the mantle temperatures are expected to be higher than 1000 K, the contribution of anharmonicity to thermodynamics of minerals of deep earth cannot be neglected. As a Mg-end-member of the olivine group and the main mineral in the upper mantle, the anharmonic properties of dry forsterite was widely studied (Gillet et al. 1991, 1997; Reynard et al. 1992). However, the anharmonicity of hydrous forsterite has not yet been reported. In this study, we carry out in situ high-temperature Raman spectroscopic investigations on a hydrous forsterite to obtain the isobaric mode Grüneisen parameters (γ_{iP}). Combined with the isothermal mode Grüneisen parameters (γ_{iT}) and thermal expansion coefficient (α) of the hydrous forsterite of the same batch reported by Ye et al. (2009) and Hushur et al. (2009), respectively, the anharmonicities of hydrous forsterite can be calculated. Then, water effect on the anharminicities can be estimated compared with the data of dry forsterite (Gillet et al. 1991, which is consistent with their later paper Gillet et al. 1997).

EXPERIMENTAL METHODS

Sample description

The hydrous forsterite single crystal (SZ0410B) was synthesized at Bayerisches Geoinstitut by Smyth et al. (2006). The synthesis was carried out in double-capsule experiments in the 5000 ton multi-anvil press at 12 GPa and 1673 K. The water content was measured by polarized FTIR spectroscopy on previously oriented grains based on the calibration of Bell et al. (2003) and the sample SZ0410B contained 4505 ppm (wt) water (Smyth et al. 2006). The size of the crystal used in this study is about 150 μm.

FTIR spectroscopy

The Mid-IR spectra (2500 to 4000 cm^{-1}) of O-H stretching vibrations before and after in situ high-temperature Raman spectroscopic study were recorded (Fig. 1) to check the retention of water during the heating process. The spectra were obtained from a Nicolet 5700 FTIR spectrometer coupled with a Continuμm microscope,

* E-mail: yanyang@ustc.edu.cn

0003-004X/15/0010–2185$05.00/DOI: http://dx.doi.org/10.2138/am-2015-5241

using a KBr beam-splitter and a liquid-nitrogen cooled MCT-A detector. All IR measurements were carried out using transmission technique. A total of 128 scans were accumulated for each spectrum at a 4 cm^{-1} resolution. The aperture size was set as 50 × 50 μm. Measurements were made under a continuous dry air flush.

In situ high-temperature Raman spectroscopy

In situ high-temperature unpolarized Raman spectroscopic investigation was conducted by use of Dilor XY micro-Raman system, with the LABRAM-HR spectrometer. The forsterite grain was placed on the sapphire window in a Linkam TS1500 heating stage. The resistance heater was used to produce high temperature, and an S type thermocouple was used to measure the sample temperature with the uncertainties of less than 1 K. The automatic temperature control unit can be programmed to set up the heating rate, desired temperature and hold time at a temperature. The sample was heated from 20 to 100 and 200 °C and then to 1000 °C at 50 °C intervals, with the heating rate of 25 °C/min. The sample was kept at every temperature for 5 min to reach thermal equilibrium.

The frequency range for the spectra was 100–1200 cm^{-1}. The sample was excited by the 514.5 nm green line of a Spectra Physics Ar ion laser. A 50× objective was used to focus the incident laser light on the sample and collect the light. The diameter of the focused laser light spot was about 10 μm. The spectrometer was calibrated using single-crystal silicon as a reference.

Data analysis

Peakfit v4.12 software was used to analyze Raman spectra at various temperatures. The obtained main frequencies and corresponding temperature derivatives are listed in Table 1. The uncertainty in the frequency is usually less than 1–3 cm^{-1} as observed by performing multiple fits on the spectra.

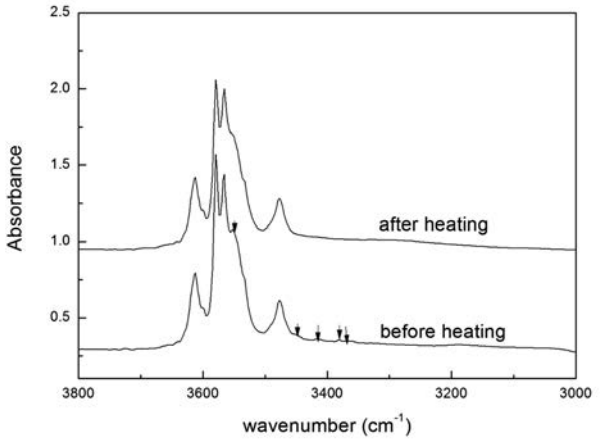

FIGURE 1. FTIR spectra of the forsterite before and after high-temperature Raman spectra measurements. The OH bands weakening or disappearing during the heating process are labeled.

RESULTS AND DISCUSSION

Figure 1 shows the absorptions of O-H stretching vibrations in forsterite before and after high-temperature Raman spectra measurement. The strong OH bands at 3613, 3579, 3566, and 3477 cm^{-1} still exist, while some weak OH bands at 3550, 3449, 3415, 3382, and 3359 cm^{-1} weaken or disappear, indicating that little dehydration occurs during the short heating process. For the total absorbance, the variation of integral absorbance from 3700 to 3100 cm^{-1} between the IR spectra before and after heating is 1.6%, suggesting little dehydration during the whole heating process. However, Ye et al. (2009) reported dehydration-breakdown of hydrous forsterite at about 900 K. The dehydration at 900 K reported by Ye et al. (2009) was assumed from the abrupt decrease in the length of b axis based on the XRD result. However, FTIR is very sensitive to O-H vibration and can directly detect the variation of OH. The little dehydration observed in this study based on the FTIR result can also be explained by the diffusion of H in forsterite. Since the diffusion of H is very slow at low temperature, we just consider the diffusion at temperatures between 600 to 1000 °C. Based on the site-specific diffusion rate of hydrogen in forsterite (Padrón-Navarta et al. 2014), the preservation of water corresponding to the OH bands at 3613, 3579, 3566, and 3477 cm^{-1} was calculated up to 99% during this short heating process with the heating rate of 25 °C/min and the hold time of 5 min at each temperature. As a result, it is not difficult to understand the preservation of the main OH bands at 3613, 3579, 3566, and 3477 cm^{-1} after the heating.

Raman modes at room temperature

It is known that in the forsterite structure, the M1 octahedron shares two edges with SiO_4 tetrahedra, whereas the M2 octahedron shares only one edge with a SiO_4 tetrahedron. In view of the greater extent of edge sharing between SiO_4 and M1 polyhedra, it is expected that the M1 cation can greatly influence the SiO_4 internal mode frequency. According to Smyth et al. (2006), the water is mainly incorporated in M1 vacancies in this forsterite, thereby water is supposed to influence the SiO_4 internal mode frequency. However, from the Raman spectrum of the hydrous forsterite at room temperature (Fig. 2), the Raman mode frequencies of this forsterite sample with 4505 ppm (wt) water agree well with the results of anhydrous forsterite and

TABLE 1. Frequencies of Raman modes, corresponding temperature derivatives, isobaric mode Grüneisen parameters, and intrinsic anharmonic parameters of hydrous and anhydrous forsterite

Symmetry	ν_i (cm^{-1})	$(\partial\nu_i/\partial T)_P$ (cm^{-1}/K)	Hydrous		Anhydrous		Mode assignment
			γ_{iP}	a_i ($10^{-5}K^{-1}$)	γ_{iP}[a]	a_i ($10^{-5}K^{-1}$)[a]	
A_g	968	−0.033	0.89	−1.16	1.07	−1.07	$SiO_4\nu_3$
B_{3g}	919	−0.034	0.97	/	0.82	−1.16	$SiO_4\nu_3$
A_g	858	−0.023	0.70	−1.04	0.72	−0.60	$SiO_4\nu_3 + \nu_1$
A_g	825	−0.022	0.70	−0.45	0.79	−0.81	$SiO_4\nu_3 + \nu_1$
A_g	610	−0.012	0.52	0.81	0.82	−0.31	$SiO_4\nu_4$
B_{3g}	590	−0.016	0.71	−0.87	0.85	−0.50	$SiO_4\nu_4$
B_{3g}	437	−0.026	1.56	−0.19	2.52	−2.38	SiO_4[b]; $SiO_4\nu_2+\nu_2$
A_g	418	−0.027	1.70	/	2.04	−2.74	$SiO_4\nu_2$
A_g	305	−0.031	2.67	−5.18	2.87	−3.22	M2[c]
A_g	227	−0.016	1.85	−4.42	1.82	−3.00	SiO_4 *t*; SiO_4 *t* + M2

Notes: γ_{iP} = corresponding to the values at 294 K, calculated following the expression $\gamma_{iP} = 1/\alpha\nu_i(\partial\nu_i/\partial T)_P$, where α is the thermal expansion coefficient. a_i = calculated following the expression $\alpha_i = \alpha(\gamma_{iT} - \gamma_{iP})$, where α is the thermal expansion coefficient.

[a] Data from Gillet et al. (1991).

[b] Indicates rotation.

[c] Indicates translation.

forsterite with 8900 ppm (wt) water (Gillet et al. 1991, 1997; Kolesov and Geiger 2004; Hushur et al. 2009; Mckeown et al. 2010), indicating water has little effect on the Raman mode frequencies at ambient conditions. For wadsleyite, Liu et al. (1998) observed a lower frequency shift about 6 cm^{-1} of most Raman modes in wadsleyite with 2.5% water and Kleppe et al. (2001) observed new Raman modes in wadsleyite with 1.65% water as compared with anhydrous wadsleyite. As a result, it is probably because that the water content up to 8900 ppm (wt) is still not enough to significantly affect the silicate framework lattice in forsterite at ambient conditions.

The lower frequencies ranging from 200 to 500 cm^{-1} are Mg2 displacements mixed with SiO_4 translations and rotations (below we use the term "lattice vibrations" to denote these low-frequency modes), the frequencies ranging from 500 to 700 cm^{-1} are SiO_4 internal bending modes, whereas the higher frequencies ranging from 800 to 1200 cm^{-1} are the SiO_4 internal stretching modes (Chopelas 1991; Kolesov and Geiger 2004; McKeown et al. 2010). The SiO_4 internal stretching modes at 968, 919, 858, and 825 cm^{-1} at room temperature are much more intense than the other modes (Fig. 2). Based on the selection rules of Raman spectroscopy, the incident light induces an instantaneous dipole moment through deforming the electron cloud around the molecule. The intensity of Raman mode depends on how easily the electron cloud can be deformed, a property measured by the polarizability. So, the intensive SiO_4 internal stretching modes suggest the highly polarizable oxygen environments.

Variations of Raman modes with increasing temperature

With increasing temperature, the Raman bands become broader, weaker, and overlapped (Fig. 2), resulting in the disappearance of the mode at 882 cm^{-1} observed at room temperature above 873 K. The evolution of the frequencies of the observed modes with temperature is illustrated in Figure 3. It is obvious in Figure 3 that all the modes shift linearly to lower wavenumbers with increasing temperature. The temperature derivatives of the Raman frequency modes

$$\left(\frac{\partial \nu_i}{\partial T}\right)_P$$

are listed in Table 1. Among the three A_g modes of SiO_4 internal stretching vibrations in this hydrous forsterite, the modes at 968 cm^{-1} observed at room temperature display the highest temperature dependences, in agreement with Gillet et al. (1991, 1997) for anhydrous forsterite. Similarly, Hushur et al. (2009) reported that this mode in hydrous forsterite showed the highest pressure dependence among the three high-frequency A_g modes of SiO_4 tetrahedra, in agreement with Chopelas (1991) for anhydrous forsterite. Hushur et al. (2009) ascribed this higher volume dependence of the mode at 968 cm^{-1} to the relatively shorter Si-O distance.

The temperature and pressure dependences of a given frequency (ν_i) result from two contributions: a pure-volume contribution due to the compressibility and thermal expansion; a pure-temperature and -pressure contribution arising from intrinsic anharmonicity (Gillet et al. 1989; Fujimori et al. 2002). As a result, the following expressions can be derived (Gillet et al. 1989; Fujimori et al. 2002; Okada et al. 2008):

$$\gamma_{iT} = \left(\frac{\partial \ln \nu_i}{\partial \rho}\right)_T = \frac{K_T}{\nu_i}\left(\frac{\partial \nu_i}{\partial P}\right)_T \quad (1)$$

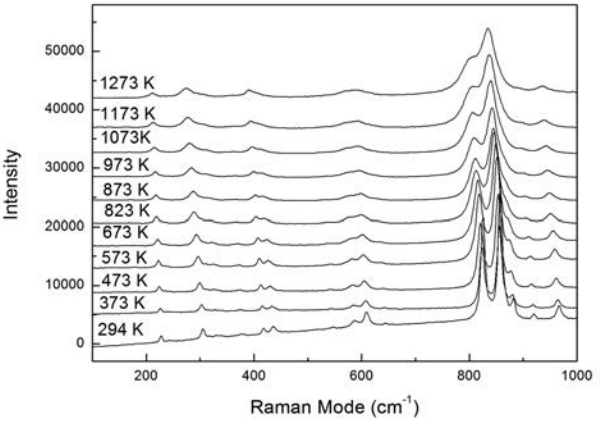

FIGURE 2. In-situ Raman spectra of forsterite up to 1273 K from 100–1200 cm^{-1}.

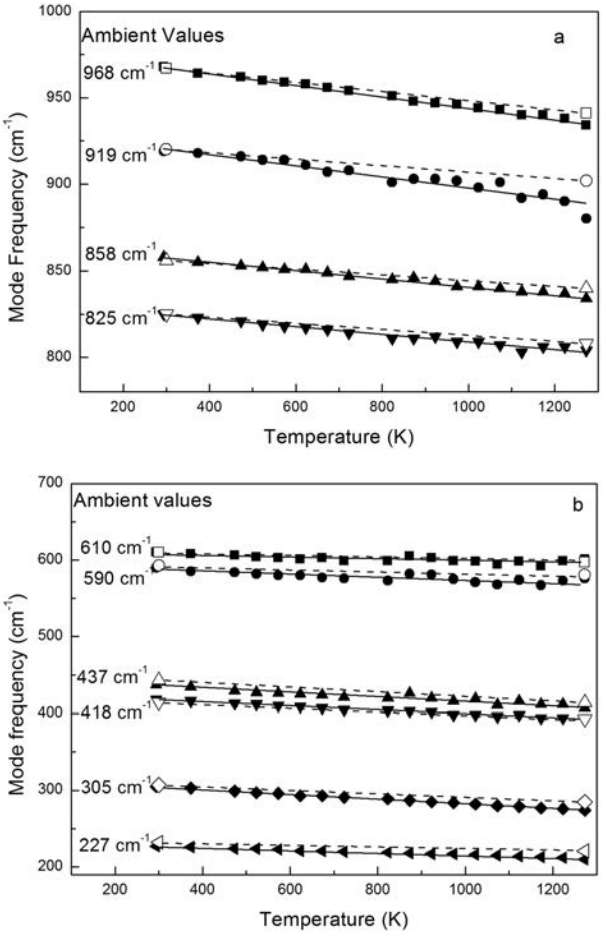

FIGURE 3. Evolutions of Raman mode frequencies of forsterite with increasing temperature for two frequency ranges: (**a**) 100–700 and (**b**) 700–1200 cm^{-1}. Solid symbols and lines are for hydrous forsterite, while open symbols and dashed lines are for anhydrous forsterite (Gillet et al. 1991).

$$\gamma_{iP} = \left(\frac{\partial \ln \nu_i}{\partial \rho}\right)_P = \frac{1}{\alpha \nu_i}\left(\frac{\partial \nu_i}{\partial T}\right)_P \quad (2)$$

$$a_i = \left(\frac{\partial \ln \nu_i}{\partial T}\right)_V = -\alpha\left(\gamma_{iP} - \gamma_{iT}\right) \quad (3)$$

where ρ is the molar density, α is the thermal expansion coefficient, K_T is the isothermal bulk modulus, γ_{iP} is the isobaric mode Grüneisen parameter, γ_{iT} is isothermal mode Grüneisen parameter, and a_i is intrinsic anharmonic parameter.

Using the obtained temperature derivatives of the Raman frequency modes at ambient pressure

$$\left(\frac{\partial \nu_i}{\partial T}\right)_P$$

and the thermal expansion coefficient (α) of hydrous forsterite reported by Ye et al. (2009), the isobaric mode Grüneisen parameters (γ_{iP}) of hydrous forsterite were calculated in Table 1 based on formula 2. Figure 4 displays the calculated isobaric mode Grüneisen parameters for various Raman frequency modes. It is evident in Figure 4 that the lattice vibration modes, especially the mode at 305 cm^{-1} related to Mg2 translation, have higher γ_{iP} values than SiO_4 internal stretching and bending modes, which is in accordance with the results of anhydrous forsterite reported by Gillet et al. (1991, 1997). This indicates that $Mg(2)O_6$ octahedron has a higher thermal expansibility than SiO_4 tetrahedron in the hydrous as well as anhydrous forsterite, which is also consistent with the results of X-ray diffraction at different temperatures of anhydrous forsterite reported by Smyth and Hazen (1973). Comparing our data with those for anhydrous forsterite (Table 1 and Fig. 5), except for the modes at 919, 858, and 227 cm^{-1}, water reduces the isobaric mode Grüneisen parameters of the Raman modes in forsterite. The effect of water on the lattice modes is slightly larger for the comparison to Gillet et al. (1991) than to Gillet et al. (1997). Therefore, water appears to influence the framework lattice modes of forsterite at high temperature. It can also be concluded from this study that water makes the $Mg(2)O_6$ octahedron less expansive. Ye et al. (2009) reported that 0.89% water increase thermal expansion coefficient of anhydrous forsterite from 36.4 to 38.1 (10^{-6} K^{-1}). The reason may be that water makes $Mg(1)O_6$ octahedron more expansive, which deserves to be tested in future by investigating water effects on the structure of forsterite at varying temperatures.

Combined with the present isobaric mode Grüneisen parameters, isothermal mode Grüneisen parameters (Hushur et al. 2009) and thermal expansion coefficient of hydrous forsterite (Ye et al. 2009), intrinsic anharmonic mode parameters of hydrous forsterite, a_i, were calculated from formula 3 and listed in Table 1. Consistent with anhydrous forsterite (Gillet et al. 1991, 1997), the intrinsic anharmonicity has a negative sign in the hydrous forsterite for most modes except for the mode at 610 cm^{-1}. However, the a_i values of the majority of Raman modes are generally greater in magnitude in the hydrous forsterite than the anhydrous one with the exception of the modes at 825 and 437 cm^{-1}, indicating the water has distinctive effect on intrinsic anharmonicity of different mode. Figure 6 compares the intrinsic anharmonic parameters of hydrous forsterite of this study and anhydrous forsterite reported by Gillet et al. (1991). It is obvious that (1) the absolute values of intrinsic anharmonic parameters related to SiO_4 internal stretching and bending vibrations are similar for both hydrous and anhydrous forsterite; (2) water has large effects on the magnitudes of anharmonic parameters related to lattice vibrations.

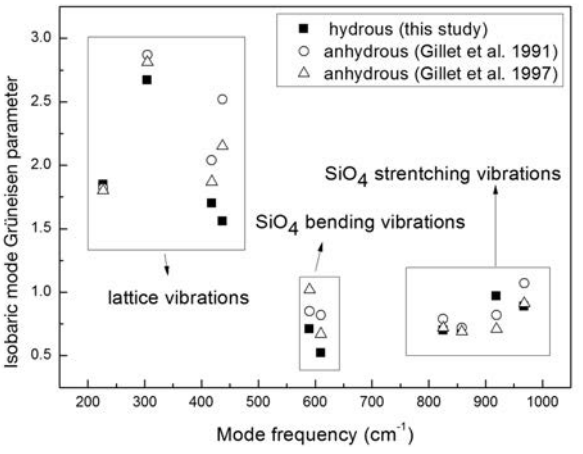

FIGURE 4. Isobaric mode Grüneisen parameters for various Raman mode frequencies in forsterite.

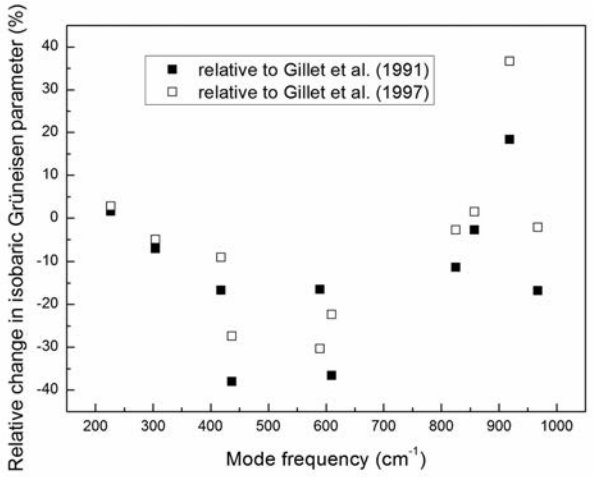

FIGURE 5. Relative changes of isobaric mode Grüneisen parameters as compared to anhydrous forsterite, which is determined by the expression, $(\gamma_{iPhydrous} - \gamma_{iPanhydrous})/\gamma_{iPanhydrous}$, where the data for anhydrous forsterite are from Gillet et al. (1991, 1997).

IMPLICATIONS

We have used in situ Raman spectra up to 1273 K to investigate the water effects on the isobaric mode Grünesien parameters and intrinsic anharmonicities of the forsterite. The results indicate that water can influence framework lattice modes of forsterite at high temperature, and the magnitudes of anharmonic parameters related to lattice vibrations. Taking the three lattice modes at 437, 305, and 227 cm^{-1} into account, the absolute values of anharmonic parameters are, on average, higher by about 0.4×10^{-5} K^{-1} than those for anhydrous

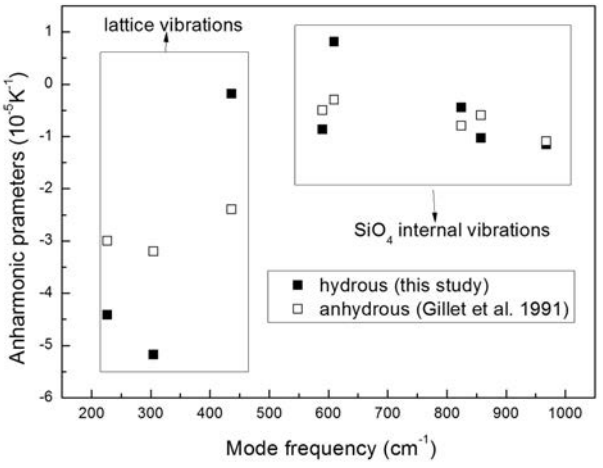

FIGURE 6. Intrinsic anharmonic parameters for various Raman mode frequencies in hydrous and anhydrous forsterite.

forsterite (Gillet et al. 1991). As stated above, anharmonicity must be considered in the case of calculation of thermodynamic functions at high temperature. Taking the calculation of isochoric heat capacity as an example, the isochoric heat capacity with the anharmonic contribution is

$$C_{\nu} = 3nR\sum_{i=1}^{m} C_{\nu i}^{h}\left(1-2a_{i}T\right) \quad (4)$$

where C_v^h is the harmonic part of the heat capacity, while the

$$-3nRT\sum_{i=1}^{m} 2a_{i}C_{\nu i}^{h}$$

is the contribution of the anharmonic properties. In the high-temperature limit ($C_{vi} \approx kT$), at which anharmonic effects become significant, formula 4 becomes

$$C_v = 3nRC_v^h(1 - 2a_{\text{avg}}T) \quad (5)$$

where a_{avg} is the arithmetic mean of the anharmonic parameters. Because the average anharmonic parameters of the three lattice modes for hydrous forsterite about 0.4×10^{-5} K^{-1} lower than for the anhydrous forsterite, the C_v corrected by the anharmonic effects of the lattice vibrations is 11% higher than for anhydrous forsterite. However, taking the mean anharmonic parameters of all the modes into account, there's little difference of C_v between hydrous and anhydrous forsterite.

Although natural olivines contain relatively little water (e.g., Bell and Rossman 1992; Peslier et al. 2002; Bell et al. 2004), these low water contents may not represent the source region because of the rapid hydrogen diffusion through olivine at high temperature especially for hydrogen incorporated in M vacancies in olivine (Demouchy et al. 2006; Padrón-Navarta et al. 2014). Numerous experiments at high temperature and pressure showed that olivine can contain considerably more water even up to 8900 ppm (wt) (Kohlstedt et al. 1996; Mosenfelder et al. 2006; Smyth et al. 2006; Férot and Bolfan-Casanova 2012). According to the previous high-pressure Raman spectroscopic studies on hydrous and anhydrous wadsleyite (Chopelas 1991; Liu et al. 1994, 1998; Kleppe et al. 2001; Yang et al. 2012), the γ_{iT} parameters are similar between hydrous wadsleyite samples with different water contents, while they are different from those of anhydrous wadsleyite. As a result, water rather than its content is significant to influence the anharmonicity of wadsleyite. It maybe suitable for forsterite, but accurate relationship between water content and the anharmonicity of olivine still should be measured to apply to the real deep mantle.

ACKNOWLEDGMENTS

This work was supported by the National Science Foundation of China (Nos. 41102024 and 41225005), the postdoctoral granted financial support from the China postdoctoral science foundation (20110490817), special financial grant from the China postdoctoral science foundation (2012T50573), and the Fundamental Research Funds for Central Universities (WK2080000029). Forsterite syntheses were supported in part by the Alexander von Humboldt Foundation and U.S. National Science Foundation grant EAR 11-13369.

REFERENCES CITED

Akimoto, S., Matsui, Y., and Syono, Y. (1976) High pressure chemistry of orthosilicate and the formation of mantle transition zone. In R.G. Strens, Ed., Physics and Chemistry of Minerals and Rocks, p. 327–363. Wiley, London.

Bell, D.R., and Rossman, G.R. (1992) Water in the Earth's mantle: the role of nominally anhydrous minerals. Science, 255, 1391–1397.

Bell, D.R., Rossman, G.R., Maldener, J., Endisch, J., and Rauch, F. (2003) Hydroxide in olivine: a quantitative determination of the absolute amount and calibration of the IR spectrum. Journal of Geophysical Research: Solid Earth, 108, 2105, http://dx.doi.org/10.1029/2001JB000679.

Bell, D.R., Rossman, G.R., and Moore, R.O. (2004) Abundance and partitioning of OH in a high pressure magmatic system: Megacrysts from Monastery kimberlite, South Africa. Journal of Petrology, 45, 1539–1564.

Beran, A., and Libowitzky, E. (2006) Water in natural mantle minerals II: Olivine, garnet and accessory minerals. In H. Keppler and J.R. Smyth, Eds., Water in Nominally Anhydrous Minerals, 62, p. 169–191. Reviews in Mineralogy and Geochemistry, Mineralogical Society of America, Chantilly, Virginia.

Bolfan-Casanova, N. (2005) Water in the Earth's mantle. Mineralogical Magazine, 69, 229–257.

Chopelas, A. (1991) Single crystal Raman spectra of forsterite, fayalite, and monticellite. American Mineralogist, 76, 1101–1109.

Demouchy, S., Jacobsen, S., Gaillard, F., and Stern, C. (2006) Rapid magma ascent recorded by water diffusion profiles in mantle olivine. Geology, 34, 429–432.

Deshpande, M.P., Bhatt, S.V., Sathe, V., Rao, R., and Chaki, S.H. (2014) Pressure and temperature dependence of Raman spectra and their anharmonic effects in Bi_2Se_3 single crystal. Physica B: Condensed Matter, 433, 72–78.

Férot, A., and Bolfan-Casanova, N. (2012) Water storage capacity in olivine and pyroxene to 14 GPa: Implications for the water content of the earth's upper mantle and nature of seismic discontinuities. Earth and Planetary Science Letters, 349-350, 218–230.

Fujimori, H., Komatsu, H., Ioku, K., and Goto, S. (2002) Anharmonic lattice mode of Ca_2SiO_4: Ultraviolet laser Raman spectroscopy at high temperatures. Physical Review B, 66, 064306.

Gillet, P., Guyot, F., and Malezieux, J.M. (1989) High-pressure, high-temperature Raman spectroscopy of Ca_2GeO_4 (olivine form): some insights on anharmonicity. Physics of the Earth and Planetary Interiors, 58, 141–154.

Gillet, P., Richet, P., Guyot, F., and Fiquet, G. (1991) High-temperature thermodynamic properties of forsterite. Journal of Geophysical Research, 96, 11805–11816.

Gillet, P., Daniel, I., and Guyot, F. (1997) Anharmonic properties of Mg2SiO4-forsterite measured from the volume dependence of the Raman spectrum. European Journal of Mineralogy, 9, 255–262.

Hirth, G., and Kohlstedt, D.L. (1996) Water in the oceanic upper mantle: implications for rheology, melt extraction and the evolution of the lithosphere. Earth and Planetary Science Letters, 144, 93–108.

Hushur, A., Manghnani, M.H., Smyth, J.R., Nestola, F., and Frost, D.J. (2009) Crystal chemistry of hydrous forsterite and its vibration properties up to 41 GPa. American Mineralogist, 94, 751–760.

Jung, H., and Karato, S. (2001) Water-induced fabric transitions in olivine. Science, 293, 1460–1493.

Karato, S.I. (2006) Influence of hydrogen-related defects on the electrical conductivity and plastic deformation of mantle minerals: a critical review. In S.D. Jacobsen and S. Van Der Lee, Eds., Earth's Deep Water Cycle, 168, p.113–129. American Geophysical Union, Washington, D.C.

Karki, B.B., Wentzcovitch, R.M., de Gironcoli, S., and Baroni, S. (2000) High-pressure lattice dynamics and thermoelasticity of MgO. Physical Review B, 61, 8793–8800.

Kieffer, S.W. (1979) Thermodynamics and lattice vibrations of minerals. 3. Lattice dynamics and an approximation for minerals with application to simple substances and framework silicates. Reviews of Geophysics and Space Physics, 17, 35–59.

Kleppe, A.K., Jephcoat, A.P., Olijnyk, H., Slesinger, A.E., Kohn, S.C., and Wood, B.J. (2001) Raman spectroscopic study of hydrous wadsleyite (β-Mg_2SiO_4) to 50 GPa. Physics and Chemistry of Minerals, 28, 232–241.

Koch-Müller, M., Matsyuk, S.S., Rhede, D., Wirth, R., and Khisina, N. (2006) Hydroxyl in mantle olivine xenocrysts from Udachnaya kimberlite pipe. Physics and Chemistry of Minerals, 33, 276–287.

Kohlstedt, D.L., Keppler, H., and Rubie, D.C. (1996) The solubility of water in α, β, and γ phases of $(Mg,Fe)_2SiO_4$. Coutributions to Mineralogy and Petrology, 123, 345–357.

Kolesov, B.A., and Geiger, C.A. (2004) A Raman spectroscopic study of Fe-Mg olivines. Physics and Chemistry of Minerals, 31, 142–154.

Liu, L.G., Mernagh, T.P., and Irfune, T. (1994) High-pressure Raman spectra of β-Mg_2SiO_4, γ-Mg_2SiO_4, $MgSiO_3$-ilmenite and $MgSiO_3$ perovskite. Journal of Physics and Chemistry of Solids, 55, 185–193.

Liu, L.G., Mernagh, T.P., Lin, C.C., Xu, J., and Inoue, T. (1998) Raman spectra of β-Mg_2SiO_4 at various pressures and temperatures. In M.H. Manghnani and T. Yagi, Eds., Properties of Earth and Planetary Materials at High Pressure and Temperature, p. 523–530. American Geophysical Union, Washington, D.C.

McKeown, D.A., Bell, M.I., and Caracas, R. (2010) Theoretical determination of the Raman spectra of single-crystal forsterite (Mg_2SiO_4). American Mineralogist, 95, 980–986.

Mosenfelder, J.L., Deligne, N.I., Asimow, P.D., and Rossman, G.R. (2006) Hydrogen incorporation in olivine from 2–12 GPa. American Mineralogist, 91, 285–294.

Mei, S., and Kohlstedt, D.L. (2000) Influence of water on plastic deformation of olivine aggregates (1): diffusion creep regimes. Journal of Geophysics Research, 105, 21457–21469.

Okada, T., Narita, T., Nagai, T., and Yamanaka, T. (2008) Comparative Raman spectroscopic study on ilmenite-type $MgSiO_3$ (akimotoite), $MgGeO_3$, and $MgTiO_3$ (geikielite) at high temperatures and high pressures. American Mineralogist, 93, 39–47.

Padrón-Navarta, J.A., Hermann, J., and O'Neill, H.St.C. (2014) Site-specific hydrogen diffusion rates in forsterite. Earth and Planetary Science Letters, 392, 100–112.

Peslier, A.H., Luhr, J.F., and Post, J. (2002) Low water content in pyroxenes from spinel-peridotites of the oxidized, sub-arc mantle wedge. Earth and Planetary Science Letters, 201, 69–86.

Reynard, B., Price, G.D., and Gillet, P. (1992) Thermodynamic and anharmonic properties of forsterite, alpha-Mg_2SiO_4-computer modeling versus high-pressure and high-temperature measurements. Journal of Geophysical Research, 97, 19,791–19,801.

Silva, A.L.C., Cândido, L., Rabelo, J.N.T., Hai, G.-Q., and Peeters, F.M. (2014) Anharmonic effects on thermodynamic properties of a grapheme monolayer. Europhysics Letters, 107, 56004, http://dx.doi.org/10.1209/0295-5075/107/56004.

Smyth, J.R., and Hazen, R.M. (1973) The crystal structures of Forsterite and Hortonolite at several temperatures up to 900 °C. American Mineralogist, 58, 588–593.

Smyth, J.R., Frost, D.J., Nestola, F., Holl, C.M., and Bromiley, G. (2006) Olivine hydration in the deep upper mantle: effects of temperature and silica activity. Geophysical Research Letters, 33, L15301.

Sumita, T., and Yoneda, A. (2014) Anharmonic effects on the equation of state (EoS) for NaCl. Physics and Chemistry of Minerals, 41, 91–103.

Wang, Q. (2010) A review of water contents and ductile deformation mechanisms of olivine: implications for the lithosphere-asthenosphere boundary of continents. Lithos, 120, 30–41.

Wu, Z. (2015) Thermodynamic properties of wadsleyite with anharmonic effect. Earthquake Science, 28, 11–16.

Yang, X., Dubrovinsky, L., Manthilake, M.A.G.M., and Wei, Q. (2012) High-pressure and high-temperature Raman spectroscopic study of hydrous wadsleyite (β-Mg_2SiO_4). Physics and Chemistry of Minerals, 39, 57–64.

Ye, Y., Schwering, R.A., and Smyth, J.R. (2009) Effect of hydration on thermal expansion of forsterite, wadsleyite and ringwoodite at ambient pressure. American Mineralogist, 94, 899–904.

Zucker, R., and Shim, S-H. (2009) In situ Raman spectroscopy of $MgSiO_3$ enstatite up to 1550 K. American Mineralogist, 94, 1638–1646.

Manuscript received November 5, 2014
Manuscript accepted April 14, 2015
Manuscript handled by Martin Kunz